J|A|C|S
ARTICLES
Published on Web 05/15/2002

Factors Governing the Protonation State of Cysteines in Proteins: An Ab Initio/CDM Study

Todor Dudev[†] and Carmay Lim*[,†,‡]

Contribution from the Institute of Biomedical Sciences, Academia Sinica, Taipei 11529, Taiwan R.O.C., and Department of Chemistry, National Tsing Hua University, Hsinchu 300, Taiwan

Received November 29, 2001. Revised Manuscript Received March 5, 2002

Abstract: The detailed mechanism of metal−cysteine binding is still poorly understood. It is not clear if every metal cation can induce cysteine deprotonation, how the dielectric medium affects this process, and the extent to which other ligands from the metal's first and second coordination shell influence cysteine ionization. It is also not clear if the zinc cation, with its positive charge reduced by charge transfer from the first two bound cysteinates, could still assist deprotonation of the next one or two cysteines in Cys_3His and Cys_4 zinc-finger cores. Here, we elucidate the factors governing the cysteine protonation state in metal-binding sites, in particular in $Zn{\cdot}Cys_4$ complexes, using a combined ab initio and continuum dielectric approach. Transition metal dications such as Zn^{2+} and Cu^{2+} and trivalent cations such as Al^{3+} with pronounced ability to accept charge from negatively charged Cys^- are predicted to induce cysteine deprotonation, but not "hard" divalent cations such as Mg^{2+}. A high dielectric medium was found to favor cysteine deprotonation, while a low one favored the protonated state. Polarizable ligands in the metal's first shell that can competitively donate charge to the metal cation were found to lower the efficiency of the metal-assisted cysteine deprotonation. The calculations predict that the zinc cation could assist deprotonation of all the cysteines during the folding of Cys_4 zinc-finger cores and the $[Zn{\cdot}(Cys^-)_4]^{2-}$ state is likely to be preserved in the final folded conformation of the protein provided the binding site is tightly encapsulated by backbone peptide groups or lysine/arginine side chains, which stabilize the ionized cysteine core.

Introduction

One-half of the 20 natural-occurring amino acids are found to participate in metal binding in proteins. Among the metal ligands, the most common coordinating groups are the side chains of histidine, cysteine, aspartic, and glutamic acid. Although binding to a metal cation induces cysteine deprotonation under physiological conditions, it is not clear (a) if every metal cation can induce cysteine deprotonation, (b) if the zinc cation, with its positive charge reduced by charge transfer from the first two bound cysteinates, could still facilitate the deprotonation of the next one or two cysteines in Cys_3His and Cys_4 zinc-finger cores, (c) how other ligands from the metal's first and second coordination shell influence cysteine ionization, and (d) how the dielectric medium affects cysteine deprotonation. Hence, in this work we have elucidated the factors governing the cysteine protonation state in metal-binding sites using a combined ab initio and continuum dielectric approach. Although emphasis has been placed on zinc−cysteine interactions, the conclusions drawn here can be applied to elucidate certain aspects of complex formation between cysteine and other transition metals of biological interest such as Cu, Ni, and Fe. The copper cation binds cysteine in azurin, pseudo-azurin, amicyanin, plastocyanin, and stellacyanin,[1] while nickel and iron complexes with cysteine(s) are observed in Ni−Fe hydrogenase[1] and the large class of iron−sulfur proteins.[2,3]

Aspartates/glutamates do not appear to be very metal-specific as they coordinate to hard (Mg^{2+}, Ca^{2+}, Mn^{2+}), borderline (Zn^{2+}, Cu^{2+}, Co^{2+}), and soft (Cd^{2+}, Hg^{2+}) metal cations.[1,4−7] At physiological pH (pH ≈ 7), aspartic acid and glutamic acid side chains that possess typical pK_a values between 4 and 5[8] would be deprotonated. These side chains tend to bind directly to the metal (inner-sphere mode) if they are located in a protein cavity or crevice with a low dielectric constant, whereas they tend to bind indirectly to the metal (outer-sphere mode) on solvent-exposed protein surfaces.[9]

Histidine side chains exhibit greater metal selectivity than carboxylates, as they prefer borderline (Zn^{2+}, Cu^{2+}, Co^{2+}, Fe^{2+}, Ni^{2+}) and soft (Cd^{2+}, Hg^{2+}) metal cations to hard ones.[1,4,7] Histidines (up to three per metal cation) are often found in metal-binding sites that play a predominantly catalytic role.[10−14]

* To whom correspondence should be addressed. E-mail: carmay@gate.sinica.edu.tw.
[†] Institute of Biomedical Sciences.
[‡] National Tsing Hua University.

(1) Rulisek, L.; Vondrasek, J. *J. Inorg. Biochem.* **1998**, *71*, 115−127.
(2) Huber, C.; Wachtershauser, G. *Science* **1998**, *281*, 670−672.
(3) Beinert, H. *J. Bioinorg. Chem.* **2000**, *5*, 2−15.
(4) Jernigan, R.; Raghunathan, G.; Bahar, I. *Curr. Opin. Struct. Biol.* **1994**, *4*, 256.
(5) Christianson, D. W.; Cox, J. D. *Annu. Rev. Biochem.* **1999**, *68*, 33−57.
(6) Dudev, T.; Cowan, J. A.; Lim, C. *J. Am. Chem. Soc.* **1999**, *121*, 7665−7673.
(7) Dudev, T.; Lin, Y. L.; Dudev, M.; Lim, C. **2002**, in preparation.
(8) Stryer, L. *Biochemistry*, 4th ed.; W. H. Freeman and Co.: New York, 1995.
(9) Dudev, T.; Lim, C. *J. Phys. Chem. B* **2000**, *104*, 3692−3694.

10.1021/ja012620l CCC: $22.00

Histidine side chains usually have pK_a values close to physiological pH,[8] but they are likely to be neutral upon binding to a positively charged metal ion. They can bind directly to metal dications (Zn^{2+}, in particular) in preformed protein cavities or on solvent-exposed surfaces.[9] Furthermore, theoretical studies suggest that a neutral histidine side chain, bridging between a metal cation and an acidic residue, may become deprotonated to an anionic imidazolate; that is, the metal-imidazole-carboxylate triad may isomerize to metal-imidazolate-carboxylic acid by transferring a proton from the imidazole ring to the carboxylate group.[15−17]

Cysteine appears to be the most enigmatic and elusive amino acid involved in metal binding. Like histidine, it prefers to bind to borderline and soft metal cations, but unlike histidine, cysteines (up to four per metal cation) are usually found in metal-binding sites that are mainly involved in protein structure stabilization as opposed to catalysis.[10−14] At physiological pH, cysteine side chains with typical pK_a values between 8 and 9[18−20] would be protonated in metal-free proteins. Binding to a metal cation (acting as a Lewis acid) causes the cysteine's pK_a to drop,[21] thus facilitating sulfhydryl group deprotonation under physiological conditions. Thus, the change in the protonation state of cysteine at neutral pH is a *metal-assisted* process.

While it is commonly accepted that the classical Zn·Cys_2-His_2 zinc-finger core is neutral, the protonation state of cysteines in zinc-finger cores containing either four cysteines[22] or a histidine and three cysteines[23] remains a subject of controversy. A consensus exists in the literature that the first two cysteines bind Zn^{2+} in an ionized form. However, current experimental data seem to present conflicting results on the protonation state of the third or fourth cysteine. From a theoretical viewpoint, it is also not certain if the zinc cation, with its positive charge reduced by charge transfer from the first two bound cysteinates, could still assist deprotonation of the next one or two cysteines. Experimental support for the deprotonation of only two cysteines comes from cobalt d−d spectroscopy and electrospray mass spectrometry. Garmer and Krauss[24] have noticed that in Co^{2+}-liver alcohol dehydrogenase the charge transfer spectrum of the structural site consisting of four cysteines is nearly identical to that of the catalytic site consisting of two cysteines, a histidine, and a water molecule, suggesting that only *two* cysteines in each site are deprotonated. Using electrospray mass spectrometry, Fabris et al.[25,26] have obtained accurate mass measurements of Cys_2His_2, Cys_3His, and Cys_4 zinc-finger peptides as well as Cys_3His and Cys_4 zinc proteins. They have concluded that only *two* of the cysteines in each binding site are ionized, while the remaining cysteine(s) appear to be protonated leading to a total charge of zero for the respective zinc complexes.

On the other hand, other experimental and theoretical data support the deprotonation of *all* metal-bound cysteines. Maynard and Covell[27] have analyzed the electrostatic screening of zinc-finger cores and have found that Cys_4 cores are much more positively screened by the protein than Cys_3His sites, which in turn are better shielded than the classical Cys_2His_2 zinc-finger cores. Hence, they have concluded that Cys_4 and Cys_3His cores are most likely anionic in the native protein; that is, all the cysteines are deprotonated. Konrat et al.[28] had earlier inferred the same conclusion from NMR analyses of the second-shell packing around Cys_3His and Cys_4 cores in quail cysteine-rich and glycine-rich CRP2 protein. Using potentiometric titration, NMR, and fluorescence spectroscopy, Bombarda et al.[20] have concluded that in aqueous solution the three cysteines in the Cys_3His motif of HIV-1 nucleocapsid protein are sequentially deprotonated in the presence of Zn^{2+}. Ryde[29] has used ab initio calculations together with X-ray data to support the deprotonation of all the cysteines in Zn·Cys_4 binding sites. In the MP2-optimized $[Zn\cdot(HS^-)_4]^{2-}$ structure, the four Zn−S^- bond distances are nearly identical (2.41 Å), whereas in the alternative structure, $[Zn\cdot(H_2S)_2\cdot(HS^-)_2]^0$, the Zn−$S^0$ (2.75 Å) and Zn−S^- (2.22 Å) distances differ by more than 0.5 Å.[29] Such inequality among the Zn−S bond distances is not observed in the X-ray structure of Cys_4 or Cys_3His zinc-finger protein, where the Zn−S distances are found within a narrow range between 2.3 and 2.4 Å,[1,7] suggesting that the zinc-bound cysteines are all deprotonated.

Here, by combining ab initio and continuum dielectric calculations, we attempt to elucidate the protonation state of cysteines in Zn·Cys_4 complexes. To this end, we have systematically assessed the effect of various factors governing the protonation state of cysteine(s) in metal-binding sites, such as the dielectric medium, the nature of the metal cation, and the effect of the other first- and second-shell ligands. The protonation state of cysteine-rich zinc cores is discussed in light of the present findings.

Methods

Models Used. Modeling cysteine as H_2S[24,29−32] or CH_3SH[24,29,32−36] has been shown to reproduce the *geometry* of zinc-cysteinate cores.[37] However, H_2S may represent cysteine better than CH_3SH in modeling reactions that affect the protonation state of cysteine since the pK_a of H_2S (6.9/7.0[38,39]) is closer to that of cysteine (8.1/8.4[18,19]) as compared to that of CH_3SH (10.3/14.2[40,41]). To verify the use of H_2S as a cysteine

(10) Vallee, B. L.; Auld, D. S. *Biochemistry* **1990**, *29*, 5647−5659.
(11) Christianson, D. W. *Adv. Protein Chem.* **1991**, *42*, 281−355.
(12) Coleman, J. E. *Annu. Rev. Biochem.* **1992**, *61*, 897−946.
(13) Lipscomb, W. N.; Strater, N. *Chem. Rev.* **1996**, *96*, 2375−2433.
(14) Berg, J. M.; Godwin, H. A. *Annu. Rev. Biophys. Biomol. Struct.* **1997**, *26*, 357.
(15) El Yazal, J.; Pang, Y.-P. *J. Phys. Chem. B* **1999**, *103*, 8773−8779.
(16) El Yazal, J.; Roe, R. R.; Pang, Y.-P. *J. Phys. Chem. B* **2000**, *104*, 6662−6667.
(17) Dudev, T.; Lim, C. *J. Phys. Chem. B* **2001**, *105*, 4446−4452.
(18) Dawson, R. M. C.; Elliot, D. C.; Elliot, W. H.; Jones, K. M. *Data for Biochemical Research*, 3rd ed.; Clarendon Press: Oxford, 1995.
(19) Lide, D. R., Ed. *Handbook of Chemistry and Physics*; CRC Press: Boca Raton, FL, 1998.
(20) Bombarda, E.; Morellet, N.; Cherradi, H.; Spiess, B.; Bouaziz, S.; Grell, E.; Roques, B. P.; Mely, Y. *J. Mol. Biol.* **2001**, *310*, 659−672.
(21) Hightower, K. E.; Huang, C.-C.; Casey, P. J.; Fierke, C. A. *Biochemistry* **1998**, *37*, 15555−15562.
(22) Petkovich, M.; Brand, N. J.; Krust, A.; Chambon, P. *Nature* **1987**, *330*, 444.
(23) Summers, M. F.; South, T. L.; Kim, B.; Hare, D. *Biochemistry* **1990**, *29*, 329.
(24) Garmer, D. R.; Krauss, M. *J. Am. Chem. Soc.* **1993**, *115*, 10247−10257.
(25) Fabris, D.; Zaia, J.; Hathout, Y.; Fenselau, C. *J. Am. Chem. Soc.* **1996**, *118*, 12242−12243.
(26) Fabris, D.; Hathout, Y.; Fenselau, C. *Inorg. Chem.* **1999**, *38*, 1322−1325.
(27) Maynard, A. T.; Covell, D. G. *J. Am. Chem. Soc.* **2001**, *123*, 1047−1058.
(28) Konrat, R.; Weiskirchen, R.; Bister, K.; Krautler, B. *J. Am. Chem. Soc.* **1998**, *120*, 7127−7128.
(29) Ryde, U. *Eur. Biophys. J.* **1996**, *24*, 213−221.
(30) Ryde, U. *Int. J. Quantum Chem.* **1994**, *52*, 1229.
(31) Deerfield, D. W., II; Pedersen, L. G. *J. Mol. Struct. (THEOCHEM)* **1997**, *419*, 221−226.
(32) Cini, R. *J. Biomol. Struct. Dyn.* **1999**, *16*, 1225−1237.
(33) Garmer, D. R.; Gresh, N. *J. Am. Chem. Soc.* **1994**, *116*, 3556−3567.
(34) Topol, I. A.; Casas-Finet, J. R.; Gussio, R.; Burt, S. K.; Erickson, J. W. *J. Mol. Struct. (THEOCHEM)* **1998**, *423*, 13−28.
(35) Topol, I. A.; Nemukhin, A. V.; Chao, M.; Iyer, L. K.; Tawa, G. J.; Burt, S. K. *J. Am. Chem. Soc.* **2000**, *122*, 7087−7094.
(36) Rulisek, L.; Havlas, Z. *J. Am. Chem. Soc.* **2000**, *122*, 10428−10439.
(37) Dudev, T.; Lim, C. *J. Phys. Chem. B* **2001**, *105*, 10709−10714.
(38) Pearson, R. G. *J. Am. Chem. Soc.* **1986**, *108*, 6109−6114.

Table 1. Calculated Solution Free Energies ΔG^{80} (in kcal/mol) for the Deprotonation Reaction $[Zn{\cdot}W_3{\cdot}LH]^{2+} \rightarrow [Zn{\cdot}W_3{\cdot}L]^{+} + H^{+}$

ligand LH	ΔG^{80}	pK_a
H_2S	−18.8	−13.8
CH_3SH	−8.8	−6.5
CH_3CH_2SH	−10.1	−7.4
$H_2N(COOH)C(H)CH_2SH$ (cysteine)	−16.0	−11.8

model for reactions involving a change in the cysteine protonation state, deprotonation free energies of different cysteine models (H_2S, CH_3SH, CH_3CH_2SH) bound to Zn^{2+} in aqueous solution were evaluated (see below) and compared with that of Zn^{2+}-bound cysteine ($H_2N(COOH)$-$C(H)CH_2SH$). The results in Table 1 show that the pK_a of the Zn^{2+}-bound H_2S (−13.8) is much closer to that of Zn^{2+}-bound cysteine (−11.8) than the pK_a values of Zn^{2+}-bound CH_3SH (−6.5) and CH_3-CH_2SH (−7.4). Because the focus of this work is on deprotonation/reprotonation of metal-free or metal-bound cysteine, the cysteine side chain was modeled by H_2S. The histidine and lysine side chains and the backbone peptide group were modeled by imidazole, $CH_3NH_3^+$, and $CH_3-CO-NH-CH_3$, respectively. As for H_2S, the experimental pK_as of imidazole (6.7/7.0[38,42]), $CH_3NH_3^+$ (10.6[42]), and $CH_3-CO-NH-CH_3$ (15.1[43]) are close to the respective values for histidine (6.5), lysine (10.5[44]), and the backbone peptide group (∼15[43]) in aqueous solution.

The preferred coordination number in zinc and copper complexes is four;[1,4,7] hence their complexes were modeled as ML_4 ($M = Zn^{2+}$, Cu^{2+}; $L = H_2O$, H_2S, HS^-, imidazole). On the other hand, magnesium and aluminum prefer to be octahedrally coordinated,[4,6,45] and their complexes were modeled as ML_6 ($M = Mg^{2+}$, Al^{3+}; $L = H_2O$, H_2S, HS^-).

Ab Initio Calculations. In a recent study,[37] we have shown that among various theoretical methods and basis sets, SVWN/6-311++G** and MP2/6-311++G**//SVWN/6-311++G** are best suited for reproducing the geometrical parameters and energetics of cysteine-like zinc complexes, respectively. Consequently, *full* geometry optimization for all the complexes studied in this work was carried out using the Gaussian 98 program[46] at the SVWN/6-311++G** level. Vibrational frequencies were then computed at the same level of theory/basis to verify that each complex was at the minimum of its potential energy surface. *No* imaginary frequency was found in any of the complexes. After scaling the frequencies by an empirical factor of 0.9833,[47] the zero-point energy (*ZPE*), thermal energy (E_T), work (*PV*), and entropy (*S*) corrections were evaluated using standard statistical mechanical formulas.[48] The electronic energies E_{elec} were then evaluated at the MP2/6-311++G**//SVWN/6-311++G** level (see above). The differences ΔE_{elec}, ΔZPE, ΔE_T, ΔPV, and ΔS between the products and reactants were employed to compute the reaction free energy at room temperature, $T = 298.15$ K, according to the following:

$$\Delta G^1 = \Delta E_{elec} + \Delta ZPE + \Delta E_T + \Delta PV - T\Delta S \qquad (1)$$

Continuum Dielectric Calculations. The reaction free energy in a given environment characterized by a dielectric constant $\epsilon = x$ can be calculated according to the following thermodynamic cycle:

$$\begin{array}{ccc} & \overset{\Delta G^1}{} & \\ \text{Reactants } (\varepsilon=1) & \rightarrow & \text{Products } (\varepsilon=1) \\ \Delta G_{solv}{}^x \text{ (Reactants)} \downarrow & & \downarrow \Delta G_{solv}{}^x \text{ (Products)} \\ \text{Reactants } (\varepsilon=x) & \underset{\Delta G^x}{\rightarrow} & \text{Products } (\varepsilon=x) \end{array}$$

ΔG^1 is the gas-phase free energy computed using eq 1. $\Delta G_{solv}{}^x$ is the free energy for transferring a molecule in the gas phase to a continuous solvent medium characterized by a dielectric constant, *x*. By solving Poisson's equation using finite difference methods[49,50] to estimate $\Delta G_{solv}{}^x$ (see below), the reaction free energy in an environment modeled by dielectric constant *x*, ΔG^x, can be computed from:

$$\Delta G^x = \Delta G^1 + \Delta G_{solv}{}^x(\text{products}) - \Delta G_{solv}{}^x(\text{reactants}) \qquad (2)$$

The continuum dielectric calculations employed a 71 × 71 × 71 lattice with an initial grid spacing 1.0 Å, and refined with a spacing of 0.25 Å, ab initio geometries, and natural bond orbital (NBO) atomic charges.[51] The low-dielectric region of the solute was defined as the region inaccessible to contact by a 1.4 Å-radius sphere rolling over the molecular surface. This region was assigned a dielectric constant of 2 ($\epsilon_{in} = 2$) to account for the electronic polarizability of the solute. The molecular surface was defined by effective solute radii, which were obtained by adjusting the CHARMM (version 22)[52] van der Waals radii to reproduce the experimental hydration free energies of the metal cations and ligands as well as the pK_a of the model ligand compounds. Some of these solute radii have been optimized in our previous study to reproduce the pK_a of H_2S, the hydration free energy of Zn^{2+}, and the reaction free energy of Zn^{2+} with 2,3-dimercapto-1-propanol.[37] These are (in Å) $R_{Zn} = 1.40$, $R_C = 1.80$, $R_S(H_2S) = 2.50$, $R_S(HS^-) = 2.29$, $R_O(H_2O) = 1.67$, $R_H(H_2O) = 0.93$, $R_H(C, H_2S) = 1.468$, $R_H(HS^-) = 1.05$. The rest of the atomic radii ($R_{Mg} = 1.50$ Å, $R_{Cu} = 1.35$ Å, $R_{Al} = 1.39$ Å, $R_O(CO) = 1.77$ Å, $R_N = 1.77$ Å, $R_H(H^+) = 0.65$ Å; R_H-(imidazole N) = 1.2 Å, R_H(amine N) = 1.1 Å, and R_H(ammonium N) = 0.93 Å) have been optimized to reproduce the experimental hydration free energies of the ions and neutral ligands as well as the pK_a values in Table 2.

Buried or partially buried metal-binding sites were characterized by an external dielectric constant ϵ_{out} equal to 2 or 4,[49,53] whereas fully solvent-exposed sites were modeled by an ϵ_{out} equal to 80. Thus, Poisson's equation was solved with ϵ_{out} equal to 1, 2, 4, or 80 and $\epsilon_{in} = 2$. The difference between the computed electrostatic potentials in a given dielectric medium ($\epsilon = x$) and in the gas phase ($\epsilon = 1$) yielded the solvation free energy $\Delta G_{solv}{}^x$ of the metal complex.

Results

Deprotonation of H_2S. The calculated enthalpies and free energies of deprotonating metal-free and metal-bound H_2S in different dielectric media are given in Table 3. In the gas phase, all of the reactions in Table 3 are enthalpy driven; the relative

(39) Atkins, P. W. *Physical Chemistry*, 6th ed.; Oxford University Press: Oxford, 1999.
(40) Howard, P. H., Meylan, W. M., Eds. *Handbook of Physical Properties of Organic Chemicals*; Lewis Publishers: Boca Raton, FL, 1997.
(41) Irving, R. J.; Nelender, L.; Wadso, I. *Acta Chem. Scand.* **1964**, *18*, 769.
(42) Smith, R. M.; Martell, A. E. *Critical Stability Constants*; Plenum Press: New York, 1989; Vol. 2, Suppl. 2.
(43) Sigel, H.; Martin, R. B. *Chem. Rev.* **1982**, *82*, 385−426.
(44) *Dictionary of Organic Compounds*, 6th ed.; Chapman & Hall: London, 1996.
(45) Marcus, Y. *Chem. Rev.* **1988**, *88*, 1475−1498.
(46) Frisch, M. J.; Trucks, G. W.; Schlegel, H. B.; Scuseria, G. E.; Robb, M. A.; Cheeseman, J. R.; Zakrzewski, V. G.; Montgomery, J. A., Jr.; Stratmann, R. E.; Burant, J. C.; Dapprich, S.; Millam, J. M.; Daniels, A. D.; Kudin, K. N.; Strain, M. C.; Farkas, O.; Tomasi, J.; Barone, V.; Cossi, M.; Cammi, R.; Mennucci, B.; Pomelli, C.; Adamo, C.; Clifford, S.; Ochterski, J.; Petersson, G. A.; Ayala, P. Y.; Cui, Q.; Morokuma, K.; Malick, D. K.; Rabuck, A. D.; Raghavachari, K.; Foresman, J. B.; Cioslowski, J.; Ortiz, J. V.; Stefanov, B. B.; Liu, G.; Liashenko, A.; Piskorz, P.; Komaromi, I.; Gomperts, R.; Martin, R. L.; Fox, D. J.; Keith, T.; Al-Laham, M. A.; Peng, C. Y.; Nanayakkara, A.; Gonzalez, C.; Challacombe, M.; Gill, P. M. W.; Johnson, B. G.; Chen, W.; Wong, M. W.; Andres, J. L.; Head-Gordon, M.; Replogle, E. S.; Pople, J. A. *Gaussian 98*, revision A.5; Gaussian, Inc.: Pittsburgh, PA, 1998.
(47) Wong, M. W. *Chem. Phys. Lett.* **1996**, *256*, 391.
(48) McQuarrie, D. A. *Statistical Mechanics*; Harper and Row: New York, 1976.
(49) Gilson, M. K.; Honig, B. *Biopolymers* **1986**, *25*, 2097.
(50) Lim, C.; Bashford, D.; Karplus, M. *J. Phys. Chem.* **1991**, *95*, 5610−5620.
(51) Reed, A. E.; Curtiss, L. A.; Weinhold, F. *Chem. Rev.* **1988**, *88*, 899−926.
(52) Brooks, B. R.; Bruccoleri, R. E.; Olafson, B. D.; States, D. J.; Swaminathan, S.; Karplus, M. *J. Comput. Chem.* **1983**, *4*, 187−217.
(53) Harvey, S. C.; Hoekstra, P. *J. Phys. Chem.* **1972**, *76*, 2987.

Table 2. Calculated Gas-Phase (ΔG^1, Eq 1) and Hydration (ΔG_{solv}^{80}) Free Energies (in kcal/mol) and pK_a Values[a]

	ΔG_{solv}^{80}		
species	calc	expt	% diff
H^+	−259.0	−262.5[a]	1.33
Mg^{2+}	−450.3	−455.5[b]	1.14
Cu^{2+}	−498.3	−498.7[b]	0.08
Al^{3+}	−1096.0	−1103.3[b]	0.66
Im	−10.5	−10.2[c]	2.94
BH → B	ΔG^{1} [d]	ΔG_{solv}^{80} [d,e]	pK_a [d]
$H_2S \rightarrow HS^-$	344.1 (345.4[f]; 345.6[g]; 347.1[h])	−0.9 (−0.7)[i]	6.7 (6.9[j]; 7.0[k])
$CH_3CONHCH_3 \rightarrow CH_3CONCH_3^-$	345.0	−10.5 (−10.0)[c]	14.1 (15.1)[l]
$CH_3NH_3^+ \rightarrow CH_3NH_2$	199.5 (205.7)[m]	−4.9 (−4.6)[n]	10.1 (10.6)[o]

[a] From Gilson and Honig, 1988.[60] [b] From Burgess, 1978.[61] [c] From Wolfenden, 1978.[62] [d] Values in parentheses are the experimental values. [e] For the deprotonation reactions, the hydration free energies of the neutral species, for which there is experimental data, are given. [f] From Rosenstock et al., 1977.[63] [g] From Cumming et al., 1978.[64] [h] From Bartmess et al., 1979.[65] [i] From Chambers et al., 1996.[66] [j] From Pearson, 1986.[38] [k] From Atkins, 1999.[39] [l] Measured for CH_3CONH_2.[43] [m] From Lias et al., 1984.[67] [n] From Cabani et al., 1981.[68] [o] From Smith and Martell, 1989.[42]

contribution of the respective entropy term to the gas-phase free energy ΔG^1 is small and positive. Ionizing metal-free hydrogen sulfide in the gas phase is very costly as evidenced by a large positive ΔG^1 of 344 kcal/mol (Table 3). Favorable solvation of the charged reaction products, particularly hydration of the small H^+ (see Table 2), substantially decreases the free energy, which drops to 9.1 kcal/mol in aqueous solution ($\epsilon = 80$). This value corresponds to a pK_a of 6.7, in close agreement with the experimental values of 6.9 and 7.0.[38,39] The positive free energies obtained for the entire range of ϵ imply that complete deprotonation of metal-free H_2S at neutral pH is unlikely regardless of the dielectric environment.

The Effect of the Metal Cation. To assess the role of the metal cation in deprotonating hydrogen sulfide, we examined the deprotonation of $M{\cdot}W_i{\cdot}H_2S$ complexes (M = Zn^{2+}, Cu^{2+}, Mg^{2+}, and Al^{3+}; W = water; i = 3 or 5, see Table 3). Upon binding to a divalent metal like Zn^{2+}, Cu^{2+}, and Mg^{2+}, the gas-phase basicity for H_2S decreases significantly (Table 3) due to stabilization of the deprotonated HS^- by the metal cation (see below). As for ΔG^1, the condensed-media ΔG^x values (x = 2, 4) for metal-bound H_2S are also less positive than the respective free energies for H_2S. Notably, the ΔG^{80} for zinc- and copper-bound H_2S becomes negative (−19 and −30 kcal/mol, respectively) in contrast to that of metal-free H_2S, but ΔG^{80} for magnesium-bound H_2S remains positive (26 kcal/mol). This implies that when cysteine, as modeled by H_2S, binds to zinc and copper on *solvent-exposed* protein surfaces, its deprotonation is thermodynamically favorable, whereas if it coordinates to magnesium, it is unlikely to be deprotonated regardless of the dielectric environment.

Because the respective complexes of the three divalent metals have the same charge for the protonated $[M{\cdot}W_i{\cdot}H_2S]^{2+}$ and deprotonated $[M{\cdot}W_i{\cdot}HS]^+$ state, their solvation free energies in a medium of dielectric constant ϵ do not differ significantly. For example, the solvation free energy difference between the deprotonated and protonated complexes of zinc, $\Delta G_{solv}^x([Zn{\cdot}W_3{\cdot}HS^-]^+) - \Delta G_{solv}^x([Zn{\cdot}W_3{\cdot}H_2S]^{2+})$, is similar to that of magnesium and is equal to 68 kcal/mol for x = 2, 102 kcal/mol for x = 4, and 135−136 kcal/mol for x = 80. Thus, it is the gas-phase free energy as opposed to solvation factors that dictates the differences among the three divalent metals.

The stability of the divalent metal complexes in the gas phase is governed not only by electrostatic interactions, but also by charge transfer from the ligand to the cation.[33] The NBO analyses carried out for the zinc, copper, and magnesium complexes reveal that the three metal ions accept the charge transferred by their ligands to varying degrees. This is evidenced in Table 4 where the effective charge on the metal cation is anticorrelated with the amount of charge transferred from the ligands to the metal. Among the metals in Table 4, copper is the best charge acceptor with the largest $CT_{L\rightarrow M}$, while magnesium is the poorest. As expected, the negatively charged HS^- transfers more charge to a given metal than does the neutral H_2S, and is therefore stabilized by a given metal more than is H_2S, as evidenced by the smaller cost of deprotonating H_2S in the gas phase when it is metal bound (Table 3). The $\Delta CT_{L\rightarrow M}$ values appear to be anticorrelated with the gas-phase deprotonation free energies: the bigger the $\Delta CT_{L\rightarrow M}$ difference, the smaller the $|\Delta G^1|$ (Table 3). Relative to neutral H_2S, the two transition metal cations (Cu^{2+} and Zn^{2+}) stabilize the deprotonated HS^- more than magnesium due mainly to stronger charge-transfer effects in the former as compared to the latter. Thus ΔG^1 for the zinc or copper complex is less positive than that for $[Mg{\cdot}W_5{\cdot}H_2S]^{2+}$ (by 43 or 76 kcal/mol).

The effect of a trivalent cation (Al^{3+}) on H_2S ionization was also studied (Table 3). As compared to the series of divalent cations, ΔH^1 and ΔG^1 for the respective aluminum-assisted reaction are much less positive due to the stronger charge−charge interaction between HS^- and the trivalent cation in $[Al{\cdot}W_5{\cdot}HS^-]^{2+}$. Solvation effects are more pronounced for the aluminum species than for the respective divalent metal complexes. The solvation free energy differences between the deprotonated and protonated aluminum complexes, $\Delta G_{solv}^x([Al{\cdot}W_5{\cdot}HS^-]^{2+}) - \Delta G_{solv}^x([Al{\cdot}W_5{\cdot}H_2S]^{3+})$, which equals 113, 170, and 225 kcal/mol for x = 2, 4, and 80, respectively, are significantly more positive than the corresponding values for the divalent metal complexes in Table 3 (see above). Consequently, despite the less positive gas-phase free energy, ΔG^{80} for the aluminum-induced H_2S deprotonation is more positive than that for the zinc- and copper-assisted processes. Nevertheless, the pK_a of $[Al{\cdot}W_5{\cdot}H_2S]^{3+}$ remains negative, indicating that trivalent Al^{3+}, like the divalent Cu^{2+} and Zn^{2+} cations, can deprotonate cysteine-like species on water-exposed surfaces.

The Effect of the First Coordination Shell Ligands. The stability of Zn^{2+} complexes with thiolate(s) is expected to depend, among other factors, on the electrostatic properties of the neighboring ligands and their ability to competitively donate charge to the metal cation (see above). To assess the role of these factors in deprotonating the zinc-bound H_2S, we examined the deprotonation of $Zn{\cdot}W_{3-i}{\cdot}L_i{\cdot}H_2S$ complexes (i = 1, 2) in which a protein ligand L (imidazole or HS^-) replaces one or two water molecules in the reference $Zn{\cdot}W_3{\cdot}H_2S$ complex (see Table 5). As compared to water, imidazole is more polarizable and donates more charge to the metal cation,[33,54] thus competing with H_2S/HS^- for Zn^{2+}. Exchanging a water molecule in $Zn{\cdot}W_3{\cdot}H_2S$ for an imidazole decreases the positive charge on zinc, which makes the metal less effective in ionizing H_2S. The $\Delta CT_{L\rightarrow M}$ drops from 0.14e in the $Zn{\cdot}W_3{\cdot}H_2S/Zn{\cdot}W_3{\cdot}(HS^-)$

(54) Dudev, T.; Lim, C. *J. Am. Chem. Soc.* **2000**, *122*, 11146−11153.

Table 3. Calculated Deprotonation ΔH^1 and ΔG^x Values (in kcal/mol) of Free and Metal-Bound H_2S for Media of Different Dielectric Constant x[a]

reaction	$\Delta CT_{L\rightarrow M}$ (e)[b]	ΔH^1	ΔG^1	ΔG^2	ΔG^4	ΔG^{80}	pK_a[c]
$H_2S \rightarrow HS^- + H^+$		350.5	344.1	188.9	104.9	9.1	6.7
$[Zn\cdot W_3\cdot H_2S]^{2+} \rightarrow [Zn\cdot W_3\cdot HS^-]^+ + H^+$	0.14	117.0	109.1	57.7	25.9	−18.8	−13.8
$[Cu\cdot W_3\cdot H_2S]^{2+} \rightarrow [Cu\cdot W_3\cdot HS^-]^+ + H^+$	0.25	82.2	76.3	32.7	6.5	−29.8	−21.9
$[Mg\cdot W_5\cdot H_2S]^{2+} \rightarrow [Mg\cdot W_5\cdot HS^-]^+ + H^+$	0.04	157.5	152.5	100.8	69.4	26.1	19.2
$[Al\cdot W_5\cdot H_2S]^{3+} \rightarrow [Al\cdot W_5\cdot HS^-]^{2+} + H^+$		31.6	24.0	17.2	8.2	−13.9	−10.2

[a] All energies in kcal/mol; $x = 1$ corresponds to gas-phase values, $x = 2$ or 4 represents buried or partially buried metal-binding sites, whereas $x = 80$ represents fully solvent-exposed sites (see Methods); W = water. The experimental hydration free energy of the proton ($\Delta G_{solv}^{80}(H^+) = -262.5$ kcal/mol) was used in computing ΔG^{80}, while the calculated $\Delta G_{solv}^4(H^+)$ of −185.3 kcal/mol and $\Delta G_{solv}^2(H^+)$ of −119.6 kcal/mol were used in evaluating ΔG^4 and ΔG^2, respectively. [b] $\Delta CT_{L\rightarrow M} = CT_{L\rightarrow M}[M\cdot W_i\cdot HS^-] - CT_{L\rightarrow M}[M\cdot W_i\cdot H_2S]$, where the $CT_{L\rightarrow M}$ values are given in Table 4. [c] Calculated values for $\epsilon = 80$.

Table 4. NBO Charges on Metal Cations (q_M) in Metal Complexes Containing Water and H_2S or HS^-

species	acceptor metal orbitals[a]	q_M (e)	$CT_{L\rightarrow M}$ (e)[b]
$[Zn\cdot W_3\cdot H_2S]^{2+}$	4s (−0.57)	1.53	0.47
$[Zn\cdot W_3\cdot HS^-]^+$		1.39	0.61
$[Cu\cdot W_3\cdot H_2S]^{2+}$	4s (−0.59)	1.17	0.83
$[Cu\cdot W_3\cdot HS^-]^+$	$3d_{yz}$ (−1.12)	0.92	1.08
$[Mg\cdot W_5\cdot H_2S]^{2+}$	3s (−0.44)	1.73	0.27
$[Mg\cdot W_5\cdot HS^-]^+$		1.69	0.31

[a] Orbital energy (in au) for the bare metal cation is given in parentheses. [b] Charge transferred from ligands to the metal cation.

couple to 0.09e in the imidazole-substituted complexes (Table 5). Consequently, the gas-phase deprotonation free energy of $Zn\cdot W_2\cdot Im\cdot H_2S$ increases by ∼21 kcal/mol relative to that of $Zn\cdot W_3\cdot H_2S$ (Table 5). This affects ΔG^x ($x = 2$, 4, or 80), which is also more positive than the respective numbers in the reference system, although ΔG^{80} remains negative indicating that the deprotonation reaction, $Zn\cdot W_2\cdot Im\cdot H_2S \rightarrow Zn\cdot W_2\cdot Im\cdot(HS^-)$, is likely to occur in aqueous solution.

The effect of the neighboring ligands on thiol deprotonation is even more pronounced when HS^- replaces one or two water molecules in $Zn\cdot W_3\cdot H_2S$. Introducing *negatively charged* residue(s) in the metal's first coordination shell greatly reduces the ability of Zn^{2+} to assist the H_2S deprotonation. This is evidenced by the significant increase in the respective gas-phase free energy: ΔG^1 increases from 109 kcal/mol for the reference $Zn\cdot W_3\cdot H_2S$ complex to 204 and 294 kcal/mol for the mono- and di-HS^- substituted complexes, respectively. As found for the metal complexes in Table 3, the observed increase in ΔG^1 in Table 5 is correlated with a drop in $\Delta CT_{L\rightarrow M}$, which decreases from 0.14e for the reference system to 0.01e and 0.005e for $Zn\cdot W_2\cdot HS^-\cdot H_2S/Zn\cdot W_2\cdot(HS^-)_2$ and $Zn\cdot W\cdot(HS^-)_2\cdot H_2S/Zn\cdot W\cdot(HS^-)_3$, respectively (Table 5). The ΔG^x ($x = 2$, 4, 80) is also more positive than the respective free energies in the reference system. However, due to the more favorable solvation of the products (especially of the proton) relative to the reactant, ΔG^{80} for the two HS^--substituted reactions remains negative implying that the deprotonation reactions may take place in aqueous solution.

Successive Deprotonation of $[Zn(H_2S)_4]^{2+}$. To assess the role of electronic and solvation factors in determining the protonation state of cysteine-rich zinc cores (see Introduction), tetrahedral zinc complexes containing a different number of thiols (H_2S) and thiolates (HS^-) were examined. H_2S is more polarizable than water but less polarizable than imidazole, and therefore its ability to donate charge to zinc is intermediate between water and imidazole.[33] Consequently, relative to $Zn\cdot W_3\cdot H_2S$, the gas-phase deprotonation free energy of $Zn(H_2S)_4$, in which three thiols have replaced three water molecules, increases slightly (by ∼4 kcal/mol, Table 6). However, solvation effects favor the deprotonated state, and hence ΔG^x ($x = 2$ and 4) is less positive, while ΔG^{80} is more negative (by ∼9 kcal/mol) than the corresponding numbers for $Zn\cdot W_3\cdot H_2S$ (compare Table 6 with Table 5).

Because of the presence of a negatively charged ligand in the first coordination shell of the metal (see above), ΔG^1 for the second deprotonation reaction increases to 205 kcal/mol even though the resulting product $[Zn\cdot(H_2S)_2\cdot(HS^-)_2]^0$ has a net charge of zero. Consequently, ΔG^{80} for the second deprotonation reaction is less favorable (−12 kcal/mol) than that for the first reaction (−28 kcal/mol), but its sign remains negative. However, the third consecutive deprotonation reaction, that is, $[Zn\cdot(H_2S)_2\cdot(HS^-)_2]^0 \rightarrow [Zn\cdot H_2S\cdot(HS^-)_3]^- + H^+$, could not be modeled since a stationary point for $[Zn\cdot H_2S\cdot(HS^-)_3]^-$ could not be located; the initial tetrahedral complex, after several steps of optimization, isomerized to a trigonal semiplanar structure with H_2S transferred to the second coordination shell. These results are in accord with previous theoretical calculations,[29] and the same result was found when H_2S was replaced by CH_3-SH. Therefore, a two-proton-release process $[Zn\cdot(H_2S)_2\cdot(HS^-)_2]^0 \rightarrow [Zn\cdot(HS^-)_4]^{2-} + 2H^+$ was considered. As expected, deprotonating neutral $[Zn\cdot(H_2S)_2\cdot(HS^-)_2]^0$ to yield a dianionic metal complex and two protons in the gas phase increases ΔG^1 substantially (to 678 kcal/mol, Table 6) relative to the first two reactions. However, the charged products are much better solvated than the neutral reactant; thus solvation effects favor ionization. The interplay between solute electronic and solvation effects results in a negative ΔG^{80} (−13 kcal/mol), implying that the last reaction, as for the first two, is thermodynamically favorable in aqueous solution.

The results presented in Table 6 suggest that the tetrathiol zinc complex could be fully deprotonated to the corresponding tetrathiolate species if the process occurs on water-exposed surfaces ($\epsilon = 80$). Low dielectric media ($\epsilon = 2-4$) characteristic of preformed solvent-inaccessible protein cavities do not seem to favor ionization of cysteine-like species, as evidenced by the large positive ΔG^2 and ΔG^4 in Table 6.

The Effect of the Second Coordination Shell Ligands. The amide backbone and the lysine and arginine side chains, which are possible proton donors, have been found to encapsulate cysteine-rich cores in zinc fingers.[27] Hence, we have explored the possibility of reprotonating $[Zn\cdot(HS^-)_4]^{2-}$ by a second-shell amide backbone (modeled by $CH_3CONHCH_3$) or a lysine side chain (modeled by $CH_3NH_3^+$) by studying $\{[Zn\cdot(HS^-)_4]\cdot(CH_3CONHCH_3)_2\}^{2-}$ and $\{[Zn\cdot(HS^-)_4]\cdot(CH_3NH_3^+)_2\}^0$ complexes in which *N*-methylacetamide and methylammonium

Table 5. Calculated Deprotonation ΔH^1 and ΔG^x Values (in kcal/mol) of Zn^{2+}-Bound H_2S Complexes for Media of Various Dielectric Constant x[a]

reaction	$\Delta CT_{L\rightarrow Zn}$ (e)[b]	ΔH^1	ΔG^1	ΔG^2	ΔG^4	ΔG^{80}	pK_a ($\epsilon = 80$)
$[Zn{\cdot}W_3{\cdot}H_2S]^{2+} \rightarrow [Zn{\cdot}W_3{\cdot}HS^-]^+ + H^+$	0.14	117.0	109.1	57.7	25.9	−18.8	−13.8
$[Zn{\cdot}W_2{\cdot}Im{\cdot}H_2S]^{2+} \rightarrow [Zn{\cdot}W_2{\cdot}Im{\cdot}HS^-]^+ + H^+$	0.09	135.6	130.3	72.8	38.2	−9.8	−7.2
$[Zn{\cdot}W_2{\cdot}HS^-{\cdot}H_2S]^+ \rightarrow [Zn{\cdot}W_2{\cdot}(HS^-)_2]^0 + H^+$	0.01	209.5	204.4	110.6	57.9	−7.2	−5.3
$[Zn{\cdot}W{\cdot}(HS^-)_2{\cdot}H_2S]^0 \rightarrow [Zn{\cdot}W{\cdot}(HS^-)_3]^- + H^+$	0.005	300.4	293.7	155.1	80.9	−2.7	−2.0

[a] See footnotes to Table 3. [b] Difference in charge transfer from ligand L to metal M: $\Delta CT_{L\rightarrow Zn} = CT_{L\rightarrow Zn}(Zn{\cdot}L_3{\cdot}HS^-) - CT_{L\rightarrow Zn}(Zn{\cdot}L_3{\cdot}H_2S)$ (L = water, imidazole, HS^-).

Table 6. Calculated Deprotonation ΔH^1 and ΔG^x Values (in kcal/mol) of H_2S in Thiol/Thiolate Zinc Complexes for Media of Different Dielectric Constant x[a]

reaction	ΔH^1	ΔG^1	ΔG^2	ΔG^4	ΔG^{80}	pK_a ($\epsilon = 80$)
$[Zn{\cdot}(H_2S)_4]^{2+} \rightarrow [Zn{\cdot}(H_2S)_3{\cdot}HS^-]^+ + H^+$	121.8	113.1	53.4	18.5	−27.7	−20.4
$[Zn{\cdot}(H_2S)_3{\cdot}HS^-]^+ \rightarrow [Zn{\cdot}(H_2S)_2{\cdot}(HS^-)_2]^0 + H^+$	210.3	204.7	107.2	53.0	−12.2	−9.0
$[Zn{\cdot}(H_2S)_2{\cdot}(HS^-)_2]^0 \rightarrow [Zn{\cdot}(HS^-)_4]^{2-} + 2H^+$	692.6	678.1	354.6	181.2	−13.0	

[a] See footnotes to Table 3.

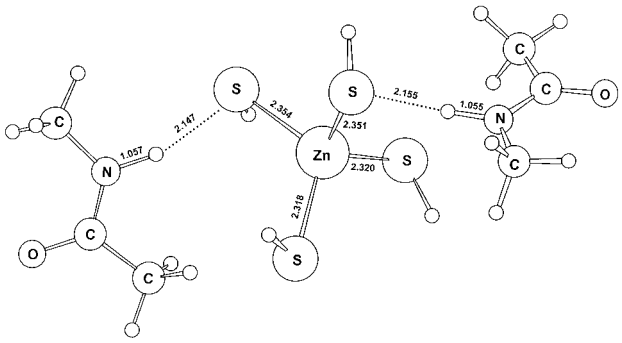

Figure 1. Ball-and-stick diagram of the fully optimized structure of the $\{[Zn{\cdot}(HS^-)_4]{\cdot}(CH_3CONHCH_3)_2\}^{2-}$ complex.

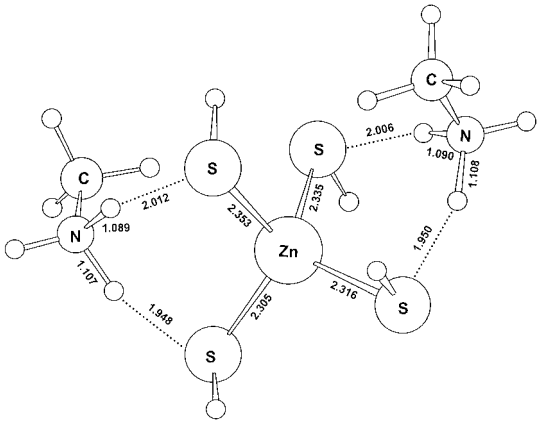

Figure 2. Ball-and-stick diagram of the fully optimized structure of the $\{[Zn{\cdot}(HS^-)_4]{\cdot}(CH_3NH_3^+)_2\}^0$ complex.

were placed in the second coordination layer (see Figures 1 and 2). Two extreme cases were considered. In the first case, the amide/ammonium proton was transferred to the first-shell thiolate sulfur by fixing R_{S-H} to 1.35 Å and $R_{H\cdots N}$ to 2.0 Å; this complex is referred to as complex I. In the second case, the proton was restrained to the second-shell amide/ammonium nitrogen by fixing R_{N-H} to 1.03 Å and $R_{H\cdots S^-}$ to 2.32 Å; this complex is referred to as complex II. Note that the N−H distance of 1.03 Å and S−H distance of 1.35 Å are typical equilibrium SVWN/6-311++G** bond distances obtained for the respective ligands. In both complexes I and II, the remaining internal coordinates were optimized. The resulting electronic energies show that complex II is more stable than the respective complex I (by 56 kcal/mol for $\{[Zn{\cdot}(HS^-)_4]{\cdot}(CH_3{-}CO{-}NH{-}CH_3)_2\}^{2-}$ and 15 kcal/mol for $\{[Zn{\cdot}(HS^-)_4]{\cdot}(CH_3NH_3^+)_2\}^0$). Thus, proton transfer from the second-shell ligand to the first-shell cysteinate seems unlikely.

Although the second-shell peptide backbone groups and lysine side chains do not seem to play a role in reprotonating the first-shell cysteinates, they can contribute to the stability of the cysteine-rich cores. To assess the extent to which the second-shell peptide backbone and lysine side chain can stabilize the zinc-finger cysteine-rich core, we evaluated the formation free energy (ΔG_{form}) of the following reactions:

$$[Zn{\cdot}(HS^-)_4]^{2-} + 2(CH_3CONHCH_3) \rightarrow \{[Zn{\cdot}(HS^-)_4]{\cdot}(CH_3CONHCH_3)_2\}^{2-} \quad (3)$$

$$[Zn{\cdot}(HS^-)_4]^{2-} + 2(CH_3NH_3^+) \rightarrow \{[Zn{\cdot}(HS^-)_4]{\cdot}(CH_3NH_3^+)_2\}^0 \quad (4)$$

The *fully* optimized structures of $\{[Zn{\cdot}(HS^-)_4]{\cdot}(CH_3CONH{-}CH_3)_2\}^{2-}$ and $\{[Zn{\cdot}(HS^-)_4]{\cdot}(CH_3NH_3^+)_2\}^0$ are shown in Figures 1 and 2, respectively. Not surprisingly, the calculated ΔG_{form} for reaction 4 (−286 kcal/mol) is much more negative than that for reaction 3 (−28 kcal/mol) due to the favorable charge−charge interactions between the negatively charged $[Zn{\cdot}(HS^-)_4]^{2-}$ and $CH_3NH_3^+$ in reaction 4. Nevertheless, the negative ΔG_{form} obtained for both reactions suggests that both backbone and lysine packing contribute significantly to the $[Zn{\cdot}(HS^-)_4]^{2-}$ core stability.

Discussion

The Interplay between Solute Electronic and Solvent Effects in Determining the Protonation State of Cysteine-like Molecules. Both solute electronic and solvent effects contribute to the protonation/deprotonation of the thiolate/thiol molecules, and the net outcome for each reaction is a delicate balance between these two effects. Solute electronic effects strongly disfavor deprotonating metal-free H_2S in the gas phase, whereas solvation (especially hydration) of the charged products, HS^- and H^+, favors the ionization process. Solvation effects, however, cannot effectively compensate for the large ΔG^1, and the free energies for deprotonating H_2S remain positive for ϵ ranging from 2 to 80 (Table 3). Binding to a metal cation

significantly decreases the gas-phase deprotonation free energy by up to 14 times (Table 3). Solvation effects in this case, however, are not as favorable as those for H_2S deprotonation since the *charged*, metal-bound reactants $[M{\cdot}W_i{\cdot}H_2S]^{2+}$ (M = Zn, Mg, Cu, Al; $i = 3$ or 5) are better solvated than neutral, metal-free H_2S. Furthermore, the favorable solvation effects are not very pronounced in low dielectric media ($\epsilon = 2-4$). Therefore, solute electronic factors dominate, and the ΔG^2 and ΔG^4 for the deprotonation reactions in Tables 3, 5, and 6 generally adopt the same positive sign as the respective ΔG^1. In aqueous solution, however, the favorable hydration free energy of the small proton (−262.5 kcal/mol) may in some cases reverse the gas-phase trends.

The interplay between solute electronic and solvent effects in determining the ionization state of H_2S is illustrated by Al^{3+}-bound H_2S. Solute electronic effects (specifically charge−charge electrostatic interactions) cause Al^{3+} to exhibit the highest ΔG^1 drop among the metals studied, but solvation effects make it less efficient in inducing H_2S deprotonation than Zn^{2+} and Cu^{2+} in aqueous solution (Table 3). Another interesting example is the stepwise deprotonation of $[Zn{\cdot}(H_2S)_4]^{2+}$. Because of the charge transfer from thiolate ligand(s), which decreases the Lewis acidity of Zn^{2+}, each successive deprotonation step is characterized by a higher *positive* ΔG^1 than its previous one (Table 6). Yet because of better solvation of the products, especially H^+, as compared to the corresponding reactant, each successive deprotonation step is characterized by more favorable solvation effects, which eventually outweigh ΔG^1 at $\epsilon = 80$. Hence, all the deprotonation reactions in Table 6 are thermodynamically favorable in aqueous solution.

Factors Governing Deprotonation/Reprotonation Processes. The metal cation plays a critical role in governing the protonation state of the cysteine-like species. By stabilizing the thiolate form, it facilitates proton release especially in high-dielectric media. Zn^{2+}, Cu^{2+}, and Al^{3+} are predicted to successfully assist thiol deprotonation on solvent-exposed surfaces (Table 3). Not any metal cation, however, can induce deprotonation. Metals, like Mg^{2+}, with low affinity toward sulfur-containing ligands and consequently limited ability to stabilize the respective thiolate complexes appear incapable of inducing H_2S deprotonation even in aqueous solution.

The dielectric medium also plays a crucial role in governing the protonation state of the cysteine-like species. The calculations suggest that deprotonation of zinc-bound H_2S generally occurs on solvent-exposed surfaces where hydration of the products, especially of H^+, favors the ionization process (Tables 5 and 6). In contrast, deprotonation of zinc-bound H_2S is unlikely to take place in the gas phase or in low dielectric media ($\epsilon \leq 4$), which favors protonation of HS^-, provided an appropriate proton donor is available nearby.

The electrostatic properties of other ligands bound to the metal can also affect the ionization of H_2S. Highly polarizable, neutral ligands (like imidazole) or negatively charged species (like HS^-) can competitively transfer charge to the metal cation, thus decreasing its Lewis acidity. This reduces the efficiency of the metal in assisting thiol ionization and results in deprotonation free energies that are more positive than the respective numbers for deprotonation of $[Zn{\cdot}W_3{\cdot}H_2S]^{2+}$ (see Table 5).

Biological Implications. The calculations predict that Zn^{2+} and Cu^{2+} can successfully aid thiol deprotonation. In fact, among all divalent metals, zinc and copper are most frequently found bound to one or more cysteines in protein-binding sites.[1,4,7,10] On the other hand, the calculations predict that Mg^{2+} cannot induce proton release from cysteine-like species. This may explain why (to the best of our knowledge) no magnesium-binding sites have been found to contain cysteine in the first coordination shell of magnesium.[6,55,56] The calculations also predict that trivalent metals such as Al^{3+} may successfully assist cysteine deprotonation. Aluminum is not a natural cofactor in proteins, and information about its binding properties is scarce. There are only three X-ray structures of aluminum-binding sites deposited in the Protein Data Bank.[57] These all are aluminum-complexed D-xylose isomerases where the natural cofactor Mg^{2+}, which is bound to Asp, Glu, and His, has been replaced by Al^{3+}. Thus it would be interesting to carry out experiments to verify if trivalent metals such as Al^{3+} could assist cysteine deprotonation.

The results obtained here suggest that all cysteines in $Zn{\cdot}Cys_4$ structural binding sites, typical of steroid receptor-type zinc fingers,[22] may become deprotonated on *solvent-exposed surfaces.* This may happen in the course of zinc-finger folding, which is known to be a metal-induced process whose initial steps involve the binding of zinc to water-accessible cysteines in the unfolded protein.[14,58,59] In the final folded structure, however, the cysteine-rich cores are usually found to be deeply buried in the protein.[7] The calculations predict that under such conditions (corresponding to a low dielectric constant), fully ionized $Zn{\cdot}(Cys^-)_4$ cores can only be preserved if they are shielded from possible proton donors. The calculations also predict that backbone peptide groups or lysine side chains in the second shell energetically stabilize tetracysteinate zinc cores, but are unlikely to reprotonate any of the Cys^-. These predictions are consistent with the finding that in zinc fingers the cysteine-rich cores are surrounded by an elaborate network of backbone:core $NH{\cdots}S^-$ hydrogen bonds, which stabilize the zinc-cysteinate structure.[27] Salt bridges formed between second-shell lysine or arginine side chains with first-shell cysteinate have been found to additionally stabilize the binding sites in some nuclear hormone receptors, Cys- and Gly-rich proteins, polymerases, and ring-finger proteins.[27,28] Taken together, these results seem to indicate that fully deprotonated $Zn{\cdot}(Cys^-)_4$ cores are likely to exist in structural binding sites provided that they are tightly encapsulated by a second coordination shell of backbone peptide groups or Lys/Arg side chains.

(55) Black, C. B.; Huang, H. W.; Cowan, J. A. *Coord. Chem. Rev.* **1994**, *135/136*, 165.
(56) Cowan, J. A. *Biological Chemistry of Magnesium*; VCH: New York, 1995.
(57) Abola, E. E.; Sussman, J. L.; Prilusky, J.; Manning, N. O. *Protein Data Bank Archives of Three-Dimensional Macromolecular Structures*; Academic Press: San Diego, 1997; Vol. 277.
(58) Miura, T.; Satoh, T.; Takeuchi, H. *Biochim. Biophys. Acta* **1998**, *1384*, 171.
(59) Krizek, B. A.; Amann, B. T.; Kilfoil, V. J.; Merkle, D. L.; Berg, J. M. *J. Am. Chem. Soc.* **1991**, *113*, 4518−4523.
(60) Gilson, M. K.; Honig, B. *Proteins: Struct., Funct., Genet.* **1988**, *4*, 7−18.
(61) Burgess, M. A. *Metal Ions in Solution*; Ellis Horwood: Chichester, England, 1978.
(62) Wolfenden, R. *Biochemistry* **1978**, *17*, 201.
(63) Rosenstock, H. M.; Draxl, K.; Steiner, B. W.; Herron, J. T. *J. Phys. Chem. Ref. Data* **1977**, *6*, 736.
(64) Cumming, J. B.; Kebarle, P. *Can. J. Chem.* **1978**, *56*, 1.
(65) Bartmess, J. E.; McIver, R. T., Jr. *Gas-Phase Ion Chemistry*; Academic Press: New York, 1979; Vol. 2.
(66) Chambers, C. C.; Hawkins, G. D.; Cramer, C. J.; Truhlar, D. G. *J. Phys. Chem.* **1996**, *100*, 16385−16398.
(67) Lias, S. G.; Liebman, J. F.; Levin, D. *J. Phys. Chem. Ref. Data* **1984**, *13*.
(68) Cabani, S.; Gianni, P.; Mollica, V.; Lepori, L. *J. Solution Chem.* **1981**, *10*, 563.

Conclusions

By using a combination of ab initio and continuum dielectric calculations, four major factors have been found to govern the protonation state of metal-bound cysteine(s) in proteins:

1. The Dielectric Medium. A high dielectric medium favors cysteine deprotonation, while a low one favors the protonated state.

2. Properties of the Metal Cation. Transition metal dications such as Zn^{2+} and Cu^{2+} with pronounced ability to accept charge from negatively charged Cys^- induce cysteine deprotonation. Trivalent cations, although rarely present as natural cofactors in proteins, are predicted to also successfully assist cysteine ionization. "Hard" divalent cations, such as Mg^{2+}, are unlikely to induce cysteine deprotonation.

3. Properties of the First-Shell Ligands. Polarizable ligands in the metal's first shell that can competitively donate charge to the metal cation lower the efficiency of the metal-assisted cysteine deprotonation.

4. Properties of the Second-Shell Ligands. Peptide backbone groups or lysine/arginine side chains in the metal's second shell can form $NH\cdots S^-$ hydrogen bonds to stabilize a negatively charged zinc-cysteinate structure.

The calculations also suggest that cysteine-rich zinc cores in proteins may be fully deprotonated if they are solvent exposed. The same protonation state $[Zn\cdot(Cys^-)_4]^{2-}$ is likely to be preserved in the final folded conformation of the protein provided the binding site is tightly encapsulated by peptide backbone groups or Lys/Arg side chains, which energetically stabilize the tetracysteinate core structure. However, in circumstances where the tight packing is compromised (by heat or chemical reagents, for example) and an appropriate proton donor is available nearby, reprotonation of first-shell cysteinate(s) in a low dielectric medium could not be ruled out.

Acknowledgment. We are grateful to D. Bashford, M. Sommer, and M. Karplus for the program to solve the Poisson equation. This work was supported by the National Science Council, Taiwan (NSC contract #90-2113-M-001), the Institute of Biomedical Sciences, and the National Center for High-Performance Computing, Taiwan.

JA012620L